Electron magnetic resonance in $La_{1-x}Ca_xMnO_3$ ($x=0.18$, 0.20, 0.22): Crossing through the boundary between ferromagnetic insulating and metallic ground states

A. I. Shames,[1,*] E. Rozenberg,[1] G. Gorodetsky,[1] and Ya. M. Mukovskii[2]
[1]*Department of Physics, Ben-Gurion University of the Negev, P.O. Box 653, 84105, Be'er-Sheva, Israel*
[2]*Moscow Steel and Alloys Institute, Leninskii prosp. 4, Moscow 117936, Russia*
(Received 28 October 2002; revised manuscript received 13 May 2003; published 3 November 2003)

Electron magnetic resonance (EMR) measurements were employed for studying the magnetic state of $La_{1-x}Ca_xMnO_3$ crystalline samples with $x=0.18$, 0.20, and 0.22. It is shown that EMR spectra of $La_{0.82}Ca_{0.18}MnO_3$ and $La_{0.8}Ca_{0.2}MnO_3$ become drastically different from those of $La_{0.78}Ca_{0.22}MnO_3$ below the Curie points of these compounds. Such spectra of $La_{0.82}Ca_{0.18}MnO_3$ and $La_{0.8}Ca_{0.2}MnO_3$ below T_C are constituted of low-intensity doublet and relatively intense singlet signals attributed to ferromagnetic insulating and ferromagnetic metallic phases, respectively. The spectra of $La_{0.78}Ca_{0.22}MnO_3$ have a shape of a broad asymmetric singlet signal similar to that observed in homogeneous ferromagnetic metallic manganites. The EMR data obtained on $La_{1-x}Ca_xMnO_3$ were compared with the recent results on magnetic, conductive, and nuclear magnetic resonance properties of these compounds and discussed in the context of transition from electronically separated phase to a homogeneous state with increasing Ca content.

DOI: 10.1103/PhysRevB.68.174402 PACS number(s): 75.30.Kz, 76.50.+g

It is well established now (see, for example, Refs. 1, 2) that substitution of La sites by Ca in parent $LaMnO_3$ compound leads to a canted antiferromagnetic insulating ground state for $x<0.1$ (x being the concentration of Ca dopant) at low temperatures (T). Further increase of Ca content in $La_{1-x}Ca_xMnO_3$ (LCMO) system results in a dominant ferromagnetic insulating (FMI) state for $0.1\leqslant x<0.22$ (Refs. 3–5) and mostly ferromagnetic metallic (FMM) ground state for $0.22<x<0.5$. Colossal magnetoresistance effect is observed in the vicinity of the Curie point T_C in this concentration interval.[1,2] It must be mentioned here that the above FMI ground state in LCMO is basically nonhomogeneous. Neutron scattering studies[3–5] provide clear evidence for the presence of FMM clusters embedded in a FMI matrix for compounds with $0.1\leqslant x\leqslant 0.2$. Other investigations of the ^{55}Mn and ^{139}La zero filed nuclear magnetic resonance (ZFNMR), as well as ac susceptibility[5–9] also suggest that for the doping range $0.1\leqslant x<0.2$ a mixed ferromagnetic ground state comprising FMI and FMM regions exists, i.e., the phase separation (PS) appears. It has been previously reported that the PS state observed in a $La_{0.82}Ca_{0.18}MnO_3$ single crystal below and above T_C manifests itself in electroresistance and magnetoresistance effects,[10] metastable conductivity,[11] ac susceptibility, and magnetization.[12] Moreover, a very recent structural study[13] of LCMO directly reveals the presence of orbitally ordered (OO) ground state in this system up to the critical concentration $x_c\sim 0.22$. Such an OO state originating from FM superexchange is responsible for the FMI phase, while FM double exchange leads to the FMM phase.[5] Thus, LCMO compounds with $x<x_c$ represent extremely complicated objects, which up to now has neither been described by consistent phenomenological nor by quantitative theoretical models. Therefore, a supplementary experimental study of LCMO system with Ca content close to x_c is extremely important. The main goal of this work is a detailed electron magnetic resonance (EMR) study of such a boundary region on the LCMO phase diagram, which can give additional insight into the magnetically ordered PS state of this system.

Prior EMR investigations of doped manganites were focused mainly on electron paramagnetic resonance (EPR) at $T>T_C$ (see, for example, Refs. 14, 15). Only a few groups[16,17] tried to analyze complicated ferromagnetic resonance (FMR) spectra of PS manganites at $T<T_C$, where different types of FM ordering occur. Our recent EMR measurements on the LCMO compound with $x=0.18$ (Ref. 12) have also demonstrated a complex structure of resonant spectra originating from the coexistence of FMI and FMM phases below T_C, and the presence of FM clusters embedded into the paramagnetic (PM) matrix above this temperature. It is reasonable to expect that a change in Ca concentration up to x_c [resulting in transition from nonhomogeneous mixed FMI-FMM to mostly FMM ground state in LCMO (Ref. 3)] must lead to notable changes in the EMR spectra of the system under consideration.

In this connection EMR study was carried out for three LCMO single crystals with $x=0.18$, 0.20, and 0.22 (marked further as $Ca_{0.18}$, $Ca_{0.20}$, and $Ca_{0.22}$, respectively). It includes monitoring of both temperature and concentration evolution of EMR spectra parameters [line shapes, resonant fields H_r, peak-to-peak linewidths ΔH_{pp}, and double integrated intensities (DIN)] that correspond to the change in the PS ground state. These measurements are complementary to a recent ZFNMR study on the LCMO system[6–8] supplying valuable information on the magnetic state for T well below T_C, while EMR also covers the FM-PM transition region and PM state. The obtained results are compared with the latest data on magnetic and conductive properties of $Ca_{0.18}$, $Ca_{0.20}$, and $Ca_{0.22}$ single crystals.[12,18]

EMR spectra were recorded using a Bruker EMX-220 X-band ($\nu=9.4$ GHz) spectrometer within the temperature range 100 K$\leqslant T\leqslant$460 K. For a detailed description of measurement technique (see Ref. 19). The measurements were carried out on loose-packed micron-sized (5–20 μm) crushed crystals. The choice in favor of loose-packed samples for EMR measurements has been argued in detail in

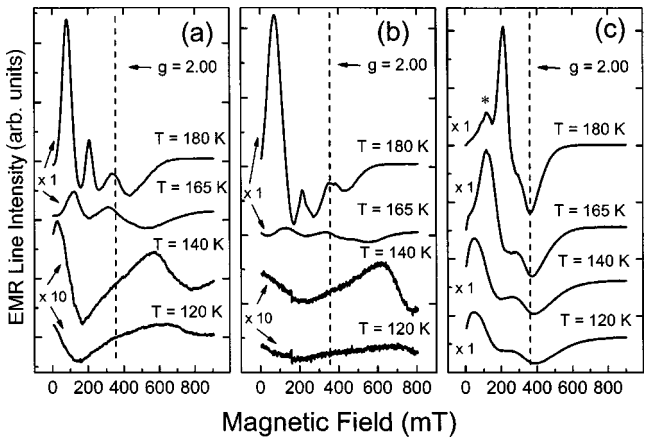

FIG. 1. EMR spectra of three manganite samples at temperatures approaching T_C from below. (a) $Ca_{0.18}$ ($\nu = 9.27$ GHz), (b) $Ca_{0.20}$ ($\nu = 9.44$ GHz), (c) $Ca_{0.22}$ ($\nu = 9.43$ GHz). In both (a) and (b) the low-temperature spectra were recorded at higher receiver gains that also revealed sharp signals at $H \sim 0.16$ T originating from the samples' holder. For all of the spectra the gain coefficients are marked at the left. The star in (c) marks a signal of the impurity ferromagnetic phase.

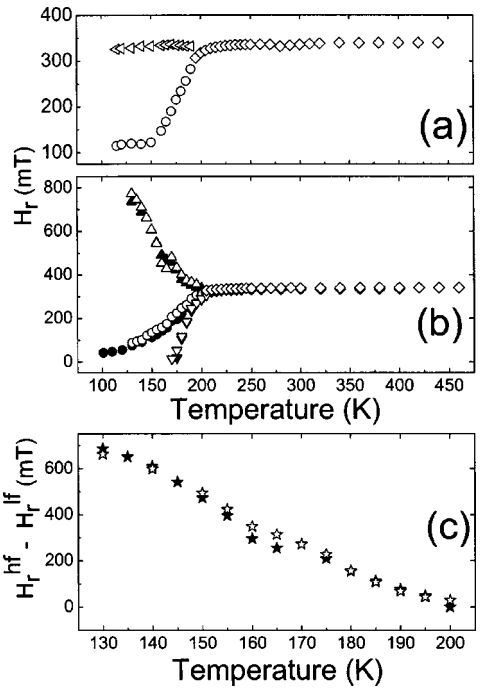

FIG. 2. Temperature dependence of the resonance fields H_r. (a) $Ca_{0.22}$, circles: main phase, FMM signal; diamonds: main phase, PM signal; triangles: impurity phase, PM signal; (b) $Ca_{0.18}$ (closed symbols) and $Ca_{0.20}$ (open symbols), circles: low field FMI signal; triangles up: high field FMI signal; triangles down: FMM-like signal; diamonds: PM signal; (c) splitting between two lines of the FMI doublet spectrum, closed stars: $Ca_{0.18}$, open stars: $Ca_{0.20}$.

Ref. 20. The crystals studied were grown by a floating zone method using radiative heating.[21] The x-ray data of the crystals were compatible with an orthorhombic unit cell of a perovskite structure. The cell parameters *a*, *b*, and *c* change in the intervals 5.5062–5.4951 Å, 7.7774–7.7814 Å, and 5.5144–5.4947 Å, respectively, with *x* changing from 0.18 to 0.22. The T_C values for $Ca_{0.18}$, $Ca_{0.20}$, and $Ca_{0.22}$ crystals are 180 ± 1, 183 ± 1, and 188 ± 1 K, respectively. It should be noted that the temperature dependences of the resistivity (ρ) upon cooling demonstrate semiconductorlike behavior at $T > T_C$, sharp maxima in the vicinity of T_C, followed by a resistivity decrease and upturn after passing local minima, observed at about 150, 140, and 135 K for $Ca_{0.18}$, $Ca_{0.20}$, and $Ca_{0.22}$ crystals, respectively. At $T \leqslant 60$ K $Ca_{0.22}$ shows metal-like conductivity, while $Ca_{0.18}$ and $Ca_{0.20}$ crystals remain insulators.[12,18] Thus, dc conductivity of the investigated crystals demonstrates a transition from predominantly nonhomogeneous FMI ground state to FMM one with increasing of Ca content from 0.18 to 0.22.

Analysis of the EMR spectra (Fig. 1) and temperature dependences of EMR parameters (Figs. 2, 3) reveals significant differences between $Ca_{0.18}$, $Ca_{0.20}$, and $Ca_{0.22}$ already at PM temperatures. Within the PM region DIN values [Fig. 3(a)] for all samples obey the Arrhenius law[19]

$$\mathrm{DIN}(T) = I_0 \exp(E_a / k_B T) \tag{1}$$

as shown in Fig. 3(b). However, the activation energy E_a in $Ca_{0.22}$ was found to be considerably higher, than in $Ca_{0.18}$ and $Ca_{0.20}$, see Table I. It is worth noting, that a similar anomaly: a jumplike change of the spin-wave stiffness coefficient *D* has already been observed in LCMO system on the crossing FMI-FMM boundary by Ca doping.[22] The linewidth ΔH_{pp} for all crystals has a pronounced minimum at $T_{\min} \sim 225$ K, see Fig. 3(c). It was found that the "bottleneck" model proposed by Shengelaya *et al.*[14] describes the $\Delta H_{pp}(T)$ dependences for these samples much better than the model of Huber *et al.*[15] The dashed line in Fig. 3(c) shows a perfect (even for temperatures approaching $T_{\min}$ from above) fit for $Ca_{0.22}$ using the equation[14]

$$\Delta H_{pp}(T) = \Delta H_0 + (A/T)\exp(-E_a / k_B T). \tag{2}$$

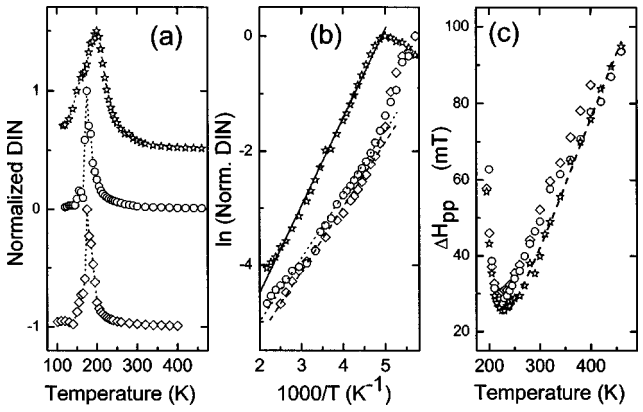

FIG. 3. Temperature dependences of EMR spectra parameters, diamonds: $Ca_{0.18}$; circles: $Ca_{0.20}$; stars: $Ca_{0.22}$: (a) double integrated intensity DIN; (b) Arrhenius plots of DIN, each line represent the best linear fit for the corresponding plot; (c) linewidth ΔH_{pp}, dashed lines represent the best fit for the $Ca_{0.22}$ sample, using the model proposed by Shengelaya *et al.* (Ref. 14).

TABLE I. Activation energies (E_a) obtained by a linear fit of ln DIN vs 1000/T plots and ΔH_{pp} vs T dependences using Eqs. (1) and (2) within the paramagnetic temperature region.

Parameter of EMR spectra used for fitting	$Ca_{0.18}$ E_a (meV)	$Ca_{0.20}$ E_a (meV)	$Ca_{0.22}$ E_a (meV)
DIN	98 ± 4	97 ± 2	132 ± 2
ΔH_{pp}	90 ± 6	87 ± 5	110 ± 6

The E_a values obtained by fitting Eq. (2) are also presented in Table I. In general, the activation energies obtained by two independent methods somehow reflect short-range correlations of a double-exchange origin in mixed-valent Mn^{3+}-Mn^{4+} clusters above T_C.[5,19] One can conclude therefore, that such intracluster interactions in $Ca_{0.22}$ are much stronger than those in $Ca_{0.18}$ and $Ca_{0.20}$.

It is not surprising that EMR in the FM region also reveals striking differences between $Ca_{0.18}$, $Ca_{0.20}$, and $Ca_{0.22}$ samples. Both $Ca_{0.18}$ and $Ca_{0.20}$ demonstrate complex EMR spectra below their Curie points. Namely, starting at $T\sim100$ K two broad lines are observed at low and high magnetic fields (H). The low field EMR signal is revealed as a resonant tail of some nonresonant microwave absorption ($H_r=0$), whereas the high field signal shows a clear maximum with H_r locating above the upper limit of the actual H scan [see lower spectra in Figs. 1(a), 1(b)]. Upon heating these lines become narrower and converge towards H_r corresponding to $g\sim2$ [see Figs. 1(a), 1(b), and 2(b)]. At $T>165$ K a third EMR line, centered at zero fields, appears. With increasing temperature this EMR signal growths, narrows, and shifts to the $g\sim2$ position, see upper spectra in Figs. 1(a), 1(b) and the $H_r(T)$ plot in Fig. 2(b). All lines merge to a single one in the vicinity of T_C, but the second derivative of the EMR spectra enables one to distinguish them up to $T\sim205$ K. Moreover, the discussed line converges into a Lorentzian-shaped one only at temperatures above $T=220$ K.

The EMR spectra of $Ca_{0.22}$ samples below T_C may be represented as a superposition of an intensive broad asymmetric line, shifted to lower fields, and a weak symmetric line with $g\sim2$ [see lower spectrum in Fig. 1(c)]. With increasing T the former line gradually narrows and shifts to a $g\sim2$ position, while the latter weakly depends on temperature. The signals merge at about 190 K and further on only the singlet line, turning to a symmetric Lorentzian-like PM signal above $T=230$ K, is observed, see Fig. 1(c). Another broad asymmetric signal [marked by a star in Fig. 1(c)] was found on the low field wing of the main signal at $T>175$ K. This signal disappears at $T\approx265$ K. Several samples, taken from different parts of the same $Ca_{0.22}$ single crystal were tested. It was found that the relative contribution of the additional signals is most pronounced for the samples originating from the edges of the crystal. This allows us to conclude that these signals result from impurity phases. One of them is PM at $T\geqslant100$ K, see the lower spectrum in Fig. 1(c) (a similar PM signal has been observed in $La_{0.7}Sr_{0.3}MnO_3$ single crystals grown by the same method[23]) and the another is FM with $T_C\approx265$ K. Both impurity phases may be due to the local nonstoichiometry of the crystal.[24]

To establish a correlation between EMR signals observed and magnetic data obtained by another techniques here we follow only a qualitative analysis based on analogies and resemblances of the EMR signals to the ones observed in well understood homogeneous systems. Indeed, such an approach significantly concedes the analysis using quantitative spectra simulations based on both spin Hamiltonians and phenomenological models. However, the extreme complexity of the PS systems under study and the lack of satisfactory magnetic resonance models for both PM and FM regions must be taken into account. The relative content of different magnetic phases in our case may vary with changing T and H making the quantitative simulations questionable. Nevertheless, the qualitative analysis done still may be useful for a better understanding of the phase separated magnetic state in the boundary region of the LCMO phase diagram.

The temperature dependent EMR spectra of $Ca_{0.18}$ and $Ca_{0.20}$ samples clearly demonstrate that two different magnetic phases are observed below T_C. Following the suggestions of Ref. 12 and observed ρ vs T dependences we may attribute the two component EMR signal observed at $T>100$ K [Figs. 1(a), 1(b), lower spectra] to the FMI phase characterized by strong nonuniaxial magnetocrystalline anisotropy which is a characteristic feature of OO FMI systems.[13] Strong anisotropy in the OO FMI phase has been also observed by the rf-enhancement technique in recent ^{139}La ZFNMR experiments.[5,8] Another FMR signal, which grows with increasing T and becomes evident at $T>165$ K resembles the EMR signal seen in homogeneous FMM manganites (see, e.g., Ref. 23). This is a reason why we attribute this signal to the FMM-like phase. In a contrast, the FMR spectra of $Ca_{0.22}$ (excluding impurity regions) show only the signal of that FMM type. The magnetic state of $Ca_{0.22}$ above 100 K may be therefore characterized as being mostly homogeneous and metallic one. The latter result is consistent with the phase diagrams of the LCMO system drawn on the basis of neutron diffraction,[3] magnetic, and ^{55}Mn ZF NMR data.[6] It is worth mentioning here that EMR reveals the presence of phase separated (FMI- and FMM-like) and homogeneous FMM states in the relevant samples at temperatures up to $1.1T_C$. Asymmetry of the PM signals resulting from the admixture of magnetically ordered phases, disappears at $T\sim1.2T_C$. Only above this temperature the magnetic state may be considered as pure PM polaronic liquidlike one.[13]

The DIN values for all samples exhibit clear maxima in the vicinity of T_C, see Fig. 3(a), $T_{max}=175$, 175, and 200 K for $Ca_{0.18}$, $Ca_{0.20}$, and $Ca_{0.22}$, respectively. Below T_{max}, DIN values for $Ca_{0.18}$ and $Ca_{0.20}$ behave in similar way. They both show a sharp drop of about two orders of magnitude when the temperature decreases towards 100 K [see Fig. 3(a) and spectra in Figs. 1(a), 1(b)]. In a marked difference the intensity of the EMR signal in $Ca_{0.22}$ decreases slowly and the line remains observable over the entire temperature range down to 100 K [see Fig. 1(c)]. Double integration of the FMI lines in the EMR spectra of $Ca_{0.18}$ and $Ca_{0.20}$, recorded at T

slightly below T_C [$T=180$ K, upper spectra in Figs. 1(a), 1(b)], allows a rough estimation of the relative volume of FMI- and FMM-like phases. For $Ca_{0.18}$ and $Ca_{0.20}$ the FMM-like phase occupies 90 and 95 % of the entire magnetic phase volumes, respectively. The above estimation provides on upper limit for the FMM-like phase content due to relatively large integration error. The phase content obtained correlates well with the data extracted from the ^{139}La ZFNMR spectra,[7] where the upper limit of the FMM phase content in $Ca_{0.20}$ was estimated to be of about 80%. In agreement with Ref. 7, we have also observed a decrease in the FMM phase content with decreasing Ca doping. All magnetic resonance data are also consistent with recent results of neutron diffraction and SANS measurements on $La_{0.9}Ca_{0.1}MnO_3$ in which the FMM phase content at low temperatures was close to 30%.[5] It is worth emphasizing here that the high content of FMM-like phase, found in $Ca_{0.18}$ and $Ca_{0.20}$, causes the metalliclike conductivity only within a narrow temperature interval below T_C, where the percolation of those FMM-like clusters occurs.[12,18] At low T, the absence of percolation of above FMM-like clusters in the FMI matrix results in the FMI ground state of $Ca_{0.18}$ and $Ca_{0.20}$ as is generally accepted for $0.1 \leqslant x < 0.22$.[3–5]

Let us discuss the unusual sharp drop of DIN below T_{max} (Fig. 3). DIN is proportional to the relative amount of the corresponding magnetic phase. On the other hand, it is proportional to the frequency dependent magnetic susceptibility of a sample. There are several possible explanations for a sharp reduction of DIN with decreasing T: (a) decrease of the actual amount of magnetic phase, (b) shift of the EMR signal to zero field (due to the increase of internal anisotropy fields), i.e., appearance of nonresonant microwave absorption (natural FMR),[25,26] and (c) appearance of so-called cluster glasslike state (CGLS), where some magnetic moments become ''frozen'' and ''invisible'' at higher frequencies, as has been earlier observed in ac susceptibility experiments.[27] Magnetization data[12,18] for the investigated samples demonstrate that for all temperatures $T<T_C$ the total volume of FM phases (FMI- and FMM-like) remains practically unchanged. Thus, only possible (b) and (c) scenarios should be taken into account. Let us consider the FMM-like phase for nonhomogeneous (FMI+FMM-like) $Ca_{0.18}$, $Ca_{0.20}$ and FMM phase for mainly homogeneous (above 100 K) FMM $Ca_{0.22}$. The above phases are the main sources of the total EMR signal for these compounds. The relevant EMR signals simultaneously sharply decrease in intensity and rapidly shift toward zero H with decreasing T. It is possible that a part of the resonant EMR absorption turns to the nonresonant one with decreasing temperature. Previously, this effect was found to be responsible for a sharp drop in low temperature microwave losses in powdered homogeneous FMM $La_{0.67}Ca_{0.33}MnO_3$.[26] Evidently, the nonresonant absorption significantly reduces the integral FMM signal intensity and may be considered as a main factor responsible for the low-T DIN behavior in $Ca_{0.22}$. However, in the case of $Ca_{0.18}$ and $Ca_{0.20}$, the CGLS effects may not be ruled out. The existence of such effects is strongly supported by the observation of frequency dependent ac susceptibility at $T<180$ K.[12,18] The justification of applying the CGLS model to FMM-like phase in low-doped LCMO ($x<x_c\sim0.22$) is provided by the results of complex studies[5] of the $x=0.1$ compound. It is claimed in Ref. 5 that in this compound the short-range ordered FMM-like clusters are embedded in a FMI matrix. The size and the relative amount of such FMM-like nonpercolative clusters were found to be 3 nm and 30%, respectively.[5] The corresponding parameters for $x=0.18$ and 0.20 were estimated as 10 nm (Refs. 12, 18) and 80–90 % just below T_C (this work and Ref. 7). Coexistence of FMM and FMI phases in a natural prerequisite for manifestations of various glassylike state effects enhancing, together with the nonresonant absorption, the reduction of DIN at $T<T_{max}$ in $Ca_{0.18}$ and $Ca_{0.20}$.

Temperature dependence of resonance fields H_r evidently reflects the changes in the magnetic anisotropy. For the FMI phase splitting between two doublet signals [Fig. 2(c)] is proportional to the ratio of the effective magnetocrystalline anisotropy constant to the magnetization. Since the magnetization in the field cooled route remains practically unchanged below T_C (Refs. 12, 18) one may conclude that the magnetic anisotropy of the FMI phase increases with decreasing temperature. The shift of the EMR line to lower H observed for the FMM-like phase with decreasing T [see Fig. 2(b)], reflects the same change of the uniaxial magnetic anisotropy. The above conclusions qualitatively agree with the ones drawn in Refs. 5, 26 for $La_{0.9}Ca_{0.1}MnO_3$ but contradict to the data on temperature dependence of the magnetic anisotropy obtained for $Ca_{0.20}$ by the rf-enhancement technique.[8] This contradiction may be due to misinterpretation of the averaged rf-enhancement factor that, in fact, must include both domain and domain wall contributions. The former directly relates to the hyperfine anisotropy field while the latter one strongly depends on the domain wall structure undergoing significant changes in $Ca_{0.20}$ when T decreases from 170 to 50 K due to angular shift of the easy magnetization axis.[18]

In summary, EMR experiments, carried out on loose packed samples originating from $La_{1-x}Ca_xMnO_3$ single crystals ($x=0.18$, 0.20, and 0.22) show significant differences in the spectra of $Ca_{0.18}$, $Ca_{0.20}$, and $Ca_{0.22}$. In the PM region ($T>T_C$) the activation energy for the dissociation of FM spin clusters is higher in $Ca_{0.22}$ (see Table I) indicating stronger intracluster double-exchange interaction in $Ca_{0.22}$ then those in $Ca_{0.18}$ and $Ca_{0.20}$. EMR spectra of $Ca_{0.18}$ and $Ca_{0.20}$ below T_C are constituted of low-intensity doublet and relatively intense singlet signal attributed to FMI and FMM-like phases, respectively. The spectra of $Ca_{0.22}$ have a shape of a broad asymmetric singlet signal similar to that observed in homogeneous FMM manganites. The sharp reduction of DIN below T_{max} is ascribed to the combined effects of FM resonant absorption changes to a non-resonant one and cluster-glass-like effects in $Ca_{0.18}$ and $Ca_{0.20}$. In the case of $Ca_{0.22}$ the nonresonant effects are the dominant ones. The magnetic anisotropy of FMI and FMM phase in $Ca_{0.18}$ and $Ca_{0.20}$ increases with T decreasing towards 100 K. These features of EMR spectra are very consistent with the model of PS ground state of $Ca_{0.18}$ and $Ca_{0.20}$, which includes orbitally ordered FMI phase and FMM-like clusters of nano-

metric size. Upon further increase of the Ca content to the critical value $x_c = 0.22$, the PS ground state changes to the FMM one. To the best of our knowledge this is the first EMR study of such a transformation in doped manganites.

We thank Professor G. Jung and Dr. M. Auslender (both at BGU) for fruitful discussions. This work was supported by the Israeli Science Foundation administered by the Israel Academy of Sciences and Humanities (Grant No. 209/01).

*Electronic address: sham@bgumail.bgu.ac.il

[1] *Colossal Magnetoresistive Oxides*, edited by Y. Tokura (Gordon and Beach Science, New York, 2000), p. 358.

[2] *Colossal Magnetoresistance, Charge Ordering and Related Properties of Manganese Oxides*, edited by C. N. R. Rao and B. Raveau (World Scientific, Singapore, 1998), p. 345.

[3] G. Biotteau, M. Hennion, F. Moussa, J. Rodriguez-Carvajal, L. Pinsard, A. Revcolevschi, Y. M. Mukovskii, and D. Shulyatev, Phys. Rev. B **64**, 104421 (2001).

[4] M. Hennion, F. Moussa, F. Wang, J. Rodriguez-Carvajal, Y. M. Mukovskii, and D. Shulyatev, cond-mat/0112159 (unpublished).

[5] P. A. Algarabel, J. M. De Teresa, J. Blasko, M. R. Ibarra, Cz. Kapusta, M. Sikora, D. Zajac, P. C. Riedi, and C. Ritter, Phys. Rev. B **67**, 134402 (2003).

[6] G. Papavassiliou, M. Fardis, M. Belesi, T. G. Maris, G. Kallias, M. Pissas, D. Niarchos, C. Dimitropolous, and J. Dolinsek, Phys. Rev. Lett. **84**, 761 (2000).

[7] G. Papavassiliou, M. Belesi, M. Fardis, and C. Dimitropoulos, Phys. Rev. Lett. **87**, 177204 (2001).

[8] M. Belesi, G. Papavassiliou, M. Fardis, M. Pissas, J. E. Wegrowe, and C. Dimitropoulos, Phys. Rev. B **63**, 180406(R) (2001).

[9] R. Laiho, E. Lahderanta, J. Salminen, K. G. Lusunov, and V. S. Zakhvalinskii, Phys. Rev. B **63**, 094405 (2001).

[10] V. Markovich, E. Rozenberg, Y. Yuzhelevski, G. Jung, G. Gorodetsky, D. A. Shulyatev, and Ya. M. Mukovskii, Appl. Phys. Lett. **78**, 3499 (2001).

[11] Y. Yuzhelevski, V. Markovich, V. Dikovsky, E. Rozenberg, G. Gorodetsky, G. Jung, D. A. Shulyatev, and Ya. M. Mukovskii, Phys. Rev. B **64**, 224428 (2002).

[12] V. Markovich, E. Rozenberg, A. I. Shames, G. Gorodetsky, I. Fita, K. Suzuki, R. Puzniak, D. A. Shulyatev, and Ya. M. Mukovskii, Phys. Rev. B **65**, 144402 (2002).

[13] B. B. Van Aken, O. D. Jurchesku, A. Meetsma, Y. Tomioka, Y. Tokura, and T. T. M. Palstra, Phys. Rev. Lett. **90**, 066403 (2003).

[14] A. Shengelaya, Guo-meng Zhao, H. Keller, K. A. Müller, and B. I. Kochelaev, Phys. Rev. B **61**, 5888 (2000).

[15] D. L. Huber, G. Alejandro, A. Caneiro, M. T. Causa, F. Prado, M. Tovar, and S. B. Oseroff, Phys. Rev. B **60**, 12 155 (1999).

[16] F. Rivadulla, M. Freita-Alvite, M. A. Lopez-Quintela, L. E. Hueso, D. R. Miguens, P. Sande, and J. Rivas, J. Appl. Phys. **91**, 785 (2002).

[17] N. V. Volkov, G. A. Petrakovskii, V. N. Vasiliev, K. A. Sablina, and K. G. Patrin, J. Magn. Magn. Mater. **258–259**, 302 (2003).

[18] V. Markovich, I. Fita, R. Puzniak, M. I. Tsindlekht, A. Wisniewski, and G. Gorodetsky, Phys. Rev. B **66**, 094409 (2002).

[19] A. I. Shames, E. Rozenberg, W. H. McCarroll, M. Greenblatt, and G. Gorodetsky, Phys. Rev. B **64**, 172401 (2001).

[20] A. I. Shames, E. Rozenberg, V. Markovich, M. Auslender, A. Yakubovsky, A. Maignan, C. Martin, B. Raveau, and G. Gorodetsky, Solid State Commun. **126**, 395 (2003).

[21] D. A. Shulyatev, A. A. Arsenov, S. G. Karabashev, and Ya. M. Mukovskii, J. Cryst. Growth **198/199**, 511 (1999).

[22] P. Dai, J. A. Fernandez-Baca, E. W. Plummer, Y. Tomioka, and Y. Tokura, Phys. Rev. B **64**, 224429 (2001).

[23] A. I. Shames, E. Rozenberg, G. Gorodetsky, A. A. Arsenov, D. A. Shulyatev, Ya. M. Mukovskii, A. Gedanken, and G. Pang, J. Appl. Phys. **91**, 7929 (2002).

[24] D. Shulyatev, S. Karabashev, A. Arsenov, Ya. Mukovskii, and S. Zverkov, J. Cryst. Growth **237/239**, 810 (2002).

[25] A. Butera, A. Fainstein, E. Winkler, J. van Tol, S. B. Oseroff, and J. Tallon, J. Appl. Phys. **89**, 7666 (2001).

[26] K. A. Yates, L. F. Cohen, C. Kapusta, P. C. Riedi, and L. Ghivelder, J. Magn. Magn. Mater. **260**, 105 (2003).

[27] D. N. H. Nam, K. Jonason, P. Nordblad, N. V. Khiem, and N. X. Phuc, Phys. Rev. B **59**, 4189 (1999).